Discriminated measures of strain and temperature in metallic specimen with embedded superimposed long and short fibre Bragg Gratings

Sébastien Triollet, Laurent Robert, Emmanuel Marin, Youcef Ouerdane

Discriminated measures of strain and temperature in metallic specimen with embedded superimposed long and short fibre Bragg Gratings

Sébastien TRIOLLET[1,2], Laurent ROBERT[2], Emmanuel MARIN[1] and Youcef OUERDANE[1]

[1] Laboratoire Hubert Curien, UMR CNRS 5516, 42000 Saint Etienne (France)
[2] Université de Toulouse; INSA, UPS, Mines Albi, ISAE; ICA (Institut Clément Ader), CROMeP; Campus Jarlard, F-81013 Albi cedex 09, France

E-mail: emmanuel.marin@univ-st-etienne.fr

Abstract. We propose a superimposed fibre Bragg gratings device to measure, localize and discriminate strain and temperature effects simultaneously for structural health monitoring purpose. Long period grating (LPG) and fibre Bragg grating (FBG) exhibit different responses to an applied solicitation, thus, strain and temperature influences can be determined separately by measuring the corresponding wavelength shifts. In this paper we present a configuration based on the use of these two gratings types: a LPG and a FBG written in the same fibre section which allows us to discriminate the contributions of these two main solicitations. The sensor is calibrated in a temperature range from 22°C to 120°C, and in a strain range from 0 to 1400 $\mu\varepsilon$. The reported errors are estimated to be within ± 0.4°C and $\pm 5\mu\varepsilon$ respectively. Our sensor is compared to the ones suggested in literature for the discrimination between strain and temperature with Bragg gratings. We propose a parameter E which allows to compare the relative uncoupling efficiency of those techniques. These sensors were embedded and tested in metallic material plates for a validation purpose of structural health monitoring.

Keywords: Bragg gratings, long period grating, bre Bragg grating, temperature strain discrimination, discrimination efciency

1. Introduction

Optical fibres are considered as novel supports to measure, localize and quantify the amplitudes of the applied solicitations especially in specific or given applications environments where the information is not so easy to access. In these conditions, the embedment of Bragg gratings based sensor can be considered as an interesting alternative in particular for structural health monitoring applications. The deported optical measurements vehicle the signatures of the applied constraints and the determination of their contributions can be deduced by using an adequate analysis of the propagated signal in the wave-guide core.

The majority of the reported approaches have relied on the use of two sensors with different sensitivities to temperature and strain. A first family is based on the use of two FBGs generally positioned in series. They can be written in two fibres of different diameters [1, 2] or in fibres of different composition, e.g. silica and plastic optical fibre [3], or also fabricated under different conditions [4]. One of the FBGs can be simply positioned in an appropriate packaging, using glass tube [5, 6], cantilever [7] or with specific assembly [8], but the obtained sensor is generally large and its spatial resolution is not satisfactory. Another approach consists in the use of two superimposed FBG written at very different wavelengths [9]. That ensures a good spatial resolution of the measurand, but the sensitivities claimed by the authors are only 15% different, which is a limitation to uncoupled strain-temperature effects.

The use of a single FBG is also possible, by considering one of the following: the induced wavelength shifts of the 1st and 2nd harmonics of the reflection spectra (see e.g. [10], [11]), the induced spectrum of a chirped FBG [12] or by using a tilted FBG [13]. The latter consists of a refractive index modulation that is simply blazed relative to the fibre axis, in order to enhance the coupling between the forward-propagating core mode and the contra-propagating cladding modes observed in the transmission spectrum, which exhibit differences in the thermal and strain sensitivities. It is also reported that the discrimination can be achieved by using high birefringence optical fibre (Hi-Bi) [14]. The birefringence induced during FBG inscription is manifested as a polarization-dependent loss (PDL). Two independent measurements of the resonance wavelength shift and the changes of PDL can discriminate the temperature and strain effects.

Another view of the problem is to consider Long Period Gratings (LPG) [15]. A LPG consists of hundreds micron period refractive index modulation written in the core of a fibre, that promotes coupling between the propagating core mode and co-propagating cladding modes. The high attenuation of the cladding modes results in the transmission spectrum of the fibre containing a series of attenuation bands, corresponding to the coupling to a different cladding mode, centered at discrete wavelengths. These attenuation bands are sensitive to the period and the length of

the LPG and to the local environment: temperature, strain, bend radius and to the refractive index of the medium surrounding the fibre [16]. Similarly to the FBGs, a number of discrimination strategies using one or several LPGs are reported in the literature. Allsop *et al* [17] shows that the sensitivity of each attenuation bands can be selected in order to find the most appropriate one for discriminate strain from temperature effects. The LPGs may be written in two different fibres types, the final sensor is obtained by splicing the fibres [18]. This specific design gives different sensitivities to temperature while they are similar for strain. The disadvantage of this technique is linked to its non-well resolved spatial area, as the measurements were obtained in two different positions. Moreover, the use of two kinds of fibres leads to an additional difficulty in the process. Some studies have been reported using both LPG and FBG spatially split [19]. Those designs affect the discrimination if applied solicitations are non-homogenous and lead to a bad spatial resolution of the measurements.

Recent developments have been set in dual period gratings to achieve simultaneous measurements. Particularly, superstructures have been reported. The technique, which mixes the use of the variation of the transmitted power and the Bragg wavelength shift [20], is easily affected by the instability of the light source. Finally, LPG pairs have recently shown their potential by acting as interferometer, whereas a large sensor size [21].

In this paper, we set out an experimental method for measuring strain and temperature applied simultaneously in a material. It consists of in-situ sensor instrumentation for extracting thermal and mechanical characteristics of the material based on a dual period fibre Bragg grating. The originality of our technique is based on two superimposed Bragg gratings (FBG + LPG), allowing a very good spatial resolution of the sensor with regard the grating length. The uncoupling efficiency of our sensor is compared to the ones proposed in literature.

In the next sections, we will develop the sensor principle, its calibration procedure, and results obtained by our embedded sensor in a metallic specimen submitted simultaneously to both strain and temperature solicitations. Note that in order to be in agreement with literature and for a better comparison we will use in this paper the microstrain units for strain instead of SI one ($1\ \mu\varepsilon = 1\mu m/m$).

2. Principle

For a fibre grating and in appropriate ranges, the shift of λ_b due to an applied strain and temperature is given by:

$$\Delta\lambda_\mathrm{b} = K_\varepsilon \Delta\varepsilon + K_\mathrm{T}\Delta T \tag{1}$$

where K_ε and K_T are the sensitivities of strain and temperature respectively, $\Delta\varepsilon$ and ΔT are the variations of strain and temperature applied to the grating and $\Delta\lambda_\mathrm{b}$ is the variation of the resonance wavelength. With only (1) the two unknown cannot be

extracted. An elegant discriminating method has been previously proposed by Wang *et al* [22]. The sensor contains two superimposed Bragg gratings: a FBG and a LPG. The two resonance wavelengths shift with different variations of strain and temperature, so the relation between $\Delta\lambda_{\mathrm{bL}}$ (for the LPG), $\Delta\lambda_{\mathrm{bF}}$ (for the FBG), temperature and strain can be expressed as:

$$\begin{bmatrix} \Delta\lambda_{\mathrm{bL}} \\ \Delta\lambda_{\mathrm{bF}} \end{bmatrix} = \begin{bmatrix} K_{\mathrm{TL}} & K_{\varepsilon\mathrm{L}} \\ K_{\mathrm{TF}} & K_{\varepsilon\mathrm{F}} \end{bmatrix} \begin{bmatrix} \Delta T \\ \Delta\varepsilon \end{bmatrix} = [K] \begin{bmatrix} \Delta T \\ \Delta\varepsilon \end{bmatrix} \tag{2}$$

where $K_{\varepsilon\mathrm{F}}$ ($K_{\varepsilon\mathrm{L}}$) and K_{TF} (K_{TL}) are respectively the strain and the temperature sensitivities of the FBG (LPG), assuming that the cross sensitivities can be neglected. It has been proved that the sensitivities of LPG and FBG are different for the same applied solicitation [23]. The solution of (2) exists if:

$$D = K_{\mathrm{TL}}.K_{\varepsilon\mathrm{F}} - K_{\varepsilon\mathrm{L}}.K_{\mathrm{TF}} \neq 0 \tag{3}$$

where D is the determinant of matrix $[K]$. Once the sensitivities coefficients are estimated by experimental calibrations, one can deduce the applied variation of strain and temperature. The dual period gratings made by Wang *et al* [22] were written with a phase mask for the FBG and an amplitude mask for the LPG. The solution proposed here is a little bit different. The gratings are photo-inscribed in a H_2-loaded Corning$^{\mathrm{TM}}$ SMF-28 fibre (1 week, 140 bars, RT). The photo-inscription of the LPG is made using point per point technique with a CW UV laser beam focused on the fibre. Then, the FBG is written, over the entire LPG's length, using a phase mask with no disassembly of the fibre. Attention is paid to write a relatively short LPG (12 mm) and a FBG with the same length in order to get a small sensor with a good spatial resolution. This particular fabrication technique allows us to combine a relative short sensor length with a good spatial localization. It also provides a better accuracy of the superposition of the two gratings and the selection of the LPG coupled mode to get the best sensitivity. The stabilization of the final component response is obtained by heat treatment in air atmosphere at 150°C for 3 hours.

The interrogation of the sensor is made by a white light OEM supercontinuum source of bandwidth > 700 nm from Leukos as a probe, and an optical spectrum analyzer (Advantest Q8384) for the detection. This set up provides a better accuracy in monitoring the spectrum due to the power and the broadband of the supercontinuum source. It also presents a great advantage in comparison to ELED sources, which has a small spectral bandwidth or to classical halogen sources which have less power. Specific routines based on a Gaussian function were developed in order to fit transmission spectra. This adjustment procedure leads to an estimation of λ_{b} shift with a resolution better than 15 pm for the LPG and 1.5 pm for the FBG. These last values are typical to the gratings used.

3. Experimental characterization

A calibration bench is specially designed to induce controlled axial strain and/or temperature to the optical fibre sensor. A schematic diagram of the experimental bench is presented in figure 1.

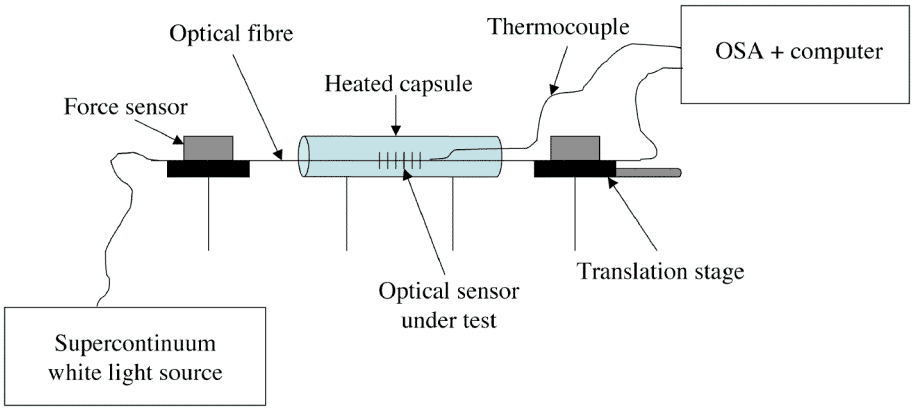

Figure 1. Schematic diagram of the calibration bench

It is composed of a 1 micrometer resolution translation stage that acts as a micro-tensile device, equipped with a force sensor of 0.24 N resolution, equivalent to 28 microstrain resolution. A micro-oven made from a heated glass capsule surroundes the optical fibre sensor. The temperature is controlled with K-thermocouples of which one of them is in the vicinity of the optical sensor, ensuring a 0.1°C resolution.

The sensitivity matrix elements of (2) are determined by measuring the wavelength shifts induced by strain and temperature separately. The temperature calibration is obtained with the heated capsule with no strain variation (the fibre was kept free at each end) [24]. Concerning the strain, the micrometric translation stage is used at fixed temperature. Figure 2 shows the evolution of the wavelength shift $\Delta\lambda_{\mathrm{bL}}$ and $\Delta\lambda_{\mathrm{bF}}$, with the applied temperature in a range of 22°C to 120°C with no applied strain. The initial Bragg wavelengths are 1293 nm for the LPG and 1533 nm for the FBG. As shown, $\Delta\lambda_{\mathrm{bL}}$ and $\Delta\lambda_{\mathrm{bF}}$ vary linearly with the temperature. The thermal sensitivities $K_{\mathrm{TL}} = 39.8$ pm/°C and $K_{\mathrm{TF}} = 13.1$ pm/°C of both the LPG and FBG are deduced from the slopes with a linear regression fit with coefficients of determination up to 0.998. The errors on the sensitivities are expressed with [25]:

$$\delta K_{\mathrm{T}j} = \left\{ \frac{1}{N-2} \left[\sum_i \left(\Delta\lambda_{\mathrm{bj_i}} - \overline{\Delta\lambda_{\mathrm{bj}}} \right)^2 - \frac{\left[\sum_i \left(T_i - \overline{T} \right) \left(\Delta\lambda_{\mathrm{bj_i}} - \overline{\Delta\lambda_{\mathrm{bj}}} \right) \right]^2}{\sum_i \left(T_i - \overline{T} \right)} \right] \right\}^{\frac{1}{2}} \tag{4}$$

with N the total number of i samples. $j = \mathrm{L}, \mathrm{F}$ stands for LPG and FBG respectively and the overline variables represents the mean value. The estimated thermal sensitivities errors lead to 0.8 pm/°C and 0.3 pm/°C for K_{TL} and K_{TF} respectively.

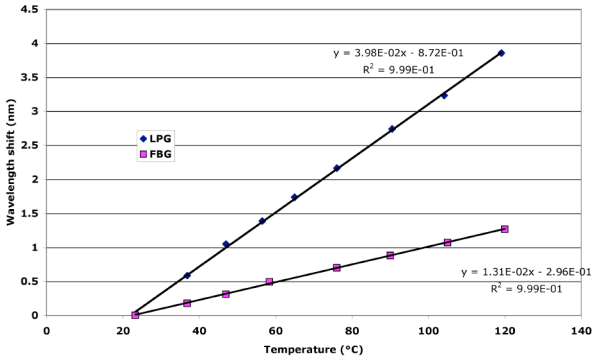

Figure 2. LPG's and FBG's wavelength shifts in air as a function of temperature T with no strain

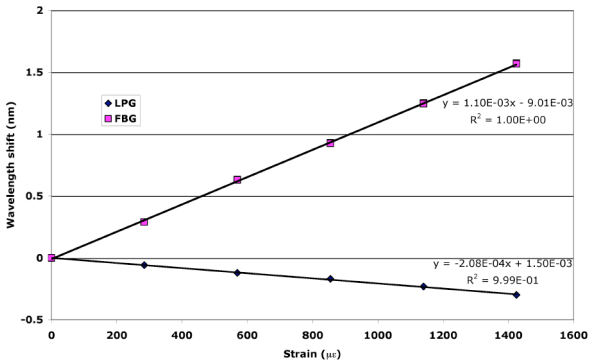

Figure 3. LPG's and FBG's wavelength shifts in air as a function of strain at 22°C

Strain is also applied to the dual period grating in a range of 0-1400 $\mu\varepsilon$ at room temperature (see Fig. 3). The deduced strain sensitivities are: $K_{\varepsilon \mathrm{L}}$ = -0.208 pm/$\mu\varepsilon$ and $K_{\varepsilon \mathrm{F}} = 1.10$ pm/$\mu\varepsilon$ respectively, with coefficients of determination up to 0.999. Using (4) while replacing temperature by strain, we found the estimated strain sensitivities errors to be 0.03 pm/$\mu\varepsilon$ and 0.01 pm/$\mu\varepsilon$ for $K_{\varepsilon \mathrm{L}}$ and $K_{\varepsilon \mathrm{F}}$ respectively. An evaluation of D from (3) leads to $D = 44\mathrm{pm}^2/^\circ\mathrm{C}/\mu\varepsilon$, this value is quite different from the ones which can be found in the literature [9]. This result is due to the opposite strain sensitivities of both gratings. However, the determinant D value does not solely allow a good estimation of the sensor discrimination quality. First, we introduce a wavelength shift vector to temperature solicitation :

$$\Delta\vec{\lambda}_{\mathrm{T}} = \left| \begin{array}{l} \Delta\lambda_{\mathrm{T_L}} = K_{\mathrm{TL}} \\ \Delta\lambda_{\mathrm{T_F}} = K_{\mathrm{TF}} \end{array} \right. \tag{5}$$

We may now define a unit vector (6):

$$\delta\vec{\lambda}_{\mathrm{T}} = \frac{\Delta\vec{\lambda}_{\mathrm{T}}}{\|\Delta\vec{\lambda}_{\mathrm{T}}\|} = \left| \begin{array}{l} K_{\mathrm{TL}}.\left(K_{\mathrm{TL}}^2 + K_{\mathrm{TF}}^2\right)^{-1/2} \\ K_{\mathrm{TF}}.\left(K_{\mathrm{TL}}^2 + K_{\mathrm{TF}}^2\right)^{-1/2} \end{array} \right. \tag{6}$$

By the same token for a strain wavelength shift vector, it follows:

$$\delta\vec{\lambda}_{\varepsilon} = \left| \begin{array}{l} K_{\varepsilon \mathrm{L}}.\left[K_{\varepsilon \mathrm{L}}^2 + K_{\varepsilon \mathrm{F}}^2\right]^{-1/2} \\ K_{\varepsilon \mathrm{F}}.\left[K_{\varepsilon \mathrm{L}}^2 + K_{\varepsilon \mathrm{F}}^2\right]^{-1/2} \end{array} \right. \tag{7}$$

With (5) to (7) we introduce a normalized parameter E to quantify how the effect of strain and temperature (applied on the sensor) are uncoupled:

$$E = |D|.\left[\left(K_{\mathrm{TL}}^2 + K_{\mathrm{TF}}^2\right).\left(K_{\varepsilon \mathrm{L}}^2 + K_{\varepsilon \mathrm{F}}^2\right)\right]^{-1/2} \tag{8}$$

The discrimination efficiency E is expressed from 0 to 1, with 1 the best temperature-strain discrimination and 0 the worst. Table 1 presents a comparison of discrimination efficiency for different discrimination techniques proposed in the literature. The discrimination efficiency E that we propose allow to compare the techniques without

taking into account the interrogation system which is usually made in literature while matching measurement errors.

Discrimination Techniques	Sensitivity matrix $[K]$	Determinant D $(pm^2/°C/\mu\varepsilon)$	Discrimination efficiency E	Reference
LPG alone	$\begin{bmatrix} 93 & 6 \\ 50 & 0.8 \end{bmatrix}$	-225.6	35%	[23]
Tilted FBG	$\begin{bmatrix} 11.1 & 0.657 \\ 11.1 & 0.766 \end{bmatrix}$	1.2099	7%	[26]
FBG with diffraction orders	$\begin{bmatrix} 11.87 & 1.203 \\ 6.604 & 0.603 \end{bmatrix}$	-0.787	4%	[27]
LPG with diffraction order	$\begin{bmatrix} -509 & 1.461 \\ -251 & 0.647 \end{bmatrix}$	37	4%	[28]
LPG in 2 fibres types	$\begin{bmatrix} 100 & 460 \\ -590 & 460 \end{bmatrix}$	317400	81%	[18]
FBG in capillary tube	$\begin{bmatrix} 9.10 & 0 \\ 9.10 & 1.23 \end{bmatrix}$	11.193	70%	[2]
Superimposed FBG/FBG	$\begin{bmatrix} 8.72 & 0.96 \\ 6.30 & 0.59 \end{bmatrix}$	-0.9032	7%	[9]
Superimposed FBG/LPG	$\begin{bmatrix} 69.4 & -0.5 \\ 10.5 & 1.1 \end{bmatrix}$	81.59	96%	[22]
Reported sensor	$\begin{bmatrix} 37.8 & -0.207 \\ 13 & 1.104 \end{bmatrix}$	44.42	99%	This work

Table 1. Comparison of discrimination efficiency for different methods proposed in the literature

Using the estimated errors on the determination of the Bragg wavelengths previously discussed ($\delta\lambda_{\mathrm{bL}} = 15$ pm and $\delta\lambda_{\mathrm{bL}} = 1.5$ pm), one can evaluate the temperature and strain measurement error due to the interrogation system [27]:

$$\begin{aligned} \delta\varepsilon_{\max} &= \pm\left[\left(\frac{K_{\varepsilon\mathrm{L}}^2}{\delta\lambda_{\mathrm{bL}}^2}+\frac{K_{\varepsilon\mathrm{F}}^2}{\delta\lambda_{\mathrm{bF}}^2}\right)-\frac{\left(\frac{K_{\varepsilon\mathrm{L}}.K_{\mathrm{TL}}}{\delta\lambda_{\mathrm{bL}}^2}+\frac{K_{\varepsilon\mathrm{F}}.K_{\mathrm{TF}}}{\delta\lambda_{\mathrm{bF}}^2}\right)^2}{\frac{K_{\mathrm{TL}}^2}{\delta\lambda_{\mathrm{bL}}^2}+\frac{K_{\mathrm{TF}}^2}{\delta\lambda_{\mathrm{bF}}^2}}\right]^{-1/2} = \pm 5\mu\varepsilon \\ \delta T_{\max} &= \pm\left[\left(\frac{K_{\mathrm{TL}}^2}{\delta\lambda_{\mathrm{bL}}^2}+\frac{K_{\mathrm{TF}}^2}{\delta\lambda_{\mathrm{bF}}^2}\right)-\frac{\left(\frac{K_{\varepsilon\mathrm{L}}.K_{\mathrm{TL}}}{\delta\lambda_{\mathrm{bL}}^2}+\frac{K_{\varepsilon\mathrm{F}}.K_{\mathrm{TF}}}{\delta\lambda_{\mathrm{bF}}^2}\right)^2}{\frac{K_{\varepsilon\mathrm{L}}^2}{\delta\lambda_{\mathrm{bL}}^2}+\frac{K_{\varepsilon\mathrm{F}}^2}{\delta\lambda_{\mathrm{bF}}^2}}\right]^{-1/2} = \pm 0.4°C \end{aligned} \tag{9}$$

These estimated errors on the discriminated measurement of strain and temperature are quite good by comparison to Brady *et al* [27]. It is worth noting that the cross sensitivities from both temperature and strain are neglected in this work. In fact, one

should consider them while it leads to a new expression of (1) from [29]:

$$\Delta\lambda_{\mathrm{b}} = K_{\varepsilon}\Delta\varepsilon + K_{\mathrm{T}}\Delta T + K_{\mathrm{T}\varepsilon}\Delta T\Delta\varepsilon \tag{10}$$

with $K_{\mathrm{T}\varepsilon}$ the temperature-strain cross sensitivities. In order to validate this hypothesis, the previous configuration was used and several strain measurements were performed at several fixed temperatures (22°C, 60°C and 88°C) for both the LPG and FBG. Figure 4 and 5 presents the calibration curves. The wavelength shift versus the strain exhibit quasi-parallel straight lines which reflects a negligible cross sensitivities in both considered solicitations. Finally, the mean value for the strain sensitivity of the LPG

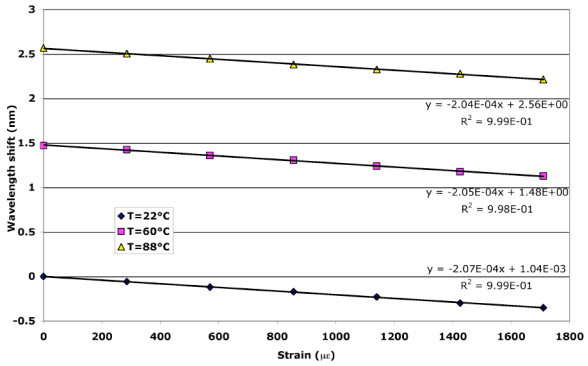

Figure 4. LPG's wavelength shift in air as a function of strain for several temperatures

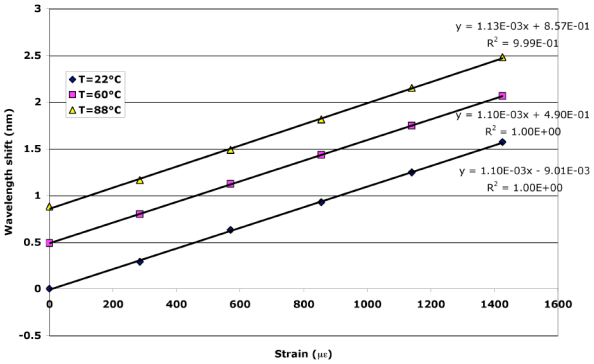

Figure 5. FBG's wavelength shift in air as a function of strain for several temperatures

over the range 22°C - 88°C is found to be $K_{\varepsilon\mathrm{L}}$ = -0.2057 pm/$\mu\varepsilon$ with a standard deviation of 0.0012 pm/$\mu\varepsilon$. For the FBG, a mean value of $K_{\varepsilon\mathrm{L}}$ = 1.1105 pm/$\mu\varepsilon$ with a standard deviation of 0.0013 pm/$\mu\varepsilon$ is reported.

4. Applications

The sensor is embedded in a groove in the middle of a steel specimen (Fig. 6). The steel specimen presents a rectangular cross-section of 10 mm x 4 mm with a length of 150 mm. The groove has a square cross-section of 1 mm^2. Embedment is made with epoxy-glue X280 from HBM on a length of 13 mm of the fiber. Strain is applied to the specimen by the use of a universal electric testing machine Instron 5800R. An aluminum cylindrical box equipped with a heating cartridge and thermocouples is used as an oven for the temperature solicitation, while strain is measured with an electric strain gauge glued on the specimen. Figure 7 shows the experimental set-up. Note that attention is paid to the thermal compensation of the strain gauge using technical specification from the manufacturer and that all sides of the heater band are closed during the measurement to guarantee the uniformity of the temperature. The applied temperature and strain are within the same range of those used for the calibration. On the one hand, the calibration results of the free sensor are compared to those of the metallic specimen ones. Nearly the same strain sensitivities for LPG and FBG are found before and after embedment,

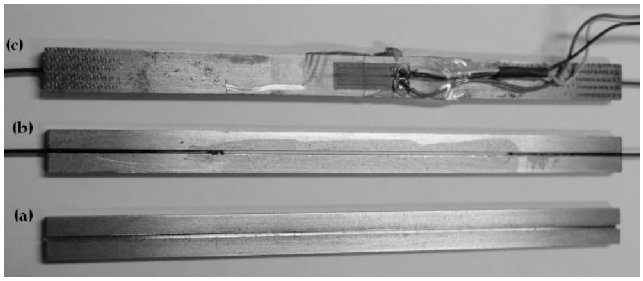

Figure 6. Metallic specimen naked (a), with Fibre sensor embedded ((b) and (c)) with a strain gauge sticks on the opposite side (c)

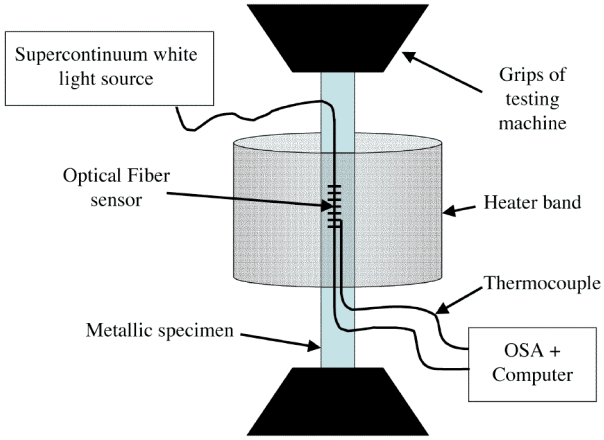

Figure 7. Schematic diagram of the metallic specimen with embedded Fiber sensor hold in strain machine and oven (all sides of the heater band are closed during the measurement to guarantee the uniformity of the temperature).

as it is shown in figure 8. This highlights the fact that the strain applied to the metallic

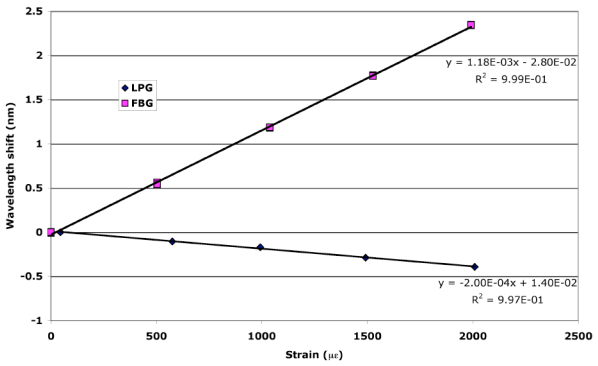

Figure 8. Wavelength shifts of embedded sensor in metallic specimen as a function of strain at 22°C

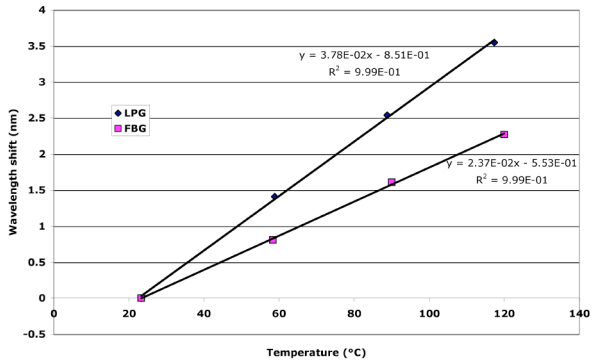

Figure 9. Wavelength shifts of embedded sensor in metallic specimen as a function of temperature with no strain

specimen is almost totally transferred to the sensor. The estimated sensitivities with the associated errors are: $K_{\varepsilon \mathrm{L}}$ = -0.199 ± 0.006 pm/$\mu\varepsilon$ and $K_{\varepsilon \mathrm{F}}$ = 1.18 ± 0.02 pm/$\mu\varepsilon$.

On the other hand, the temperature sensitivity is (see figure 9): $K^*_{\mathrm{TL}} = 37.8$ pm/°C and $K^*_{\mathrm{TF}} = 23.7$ pm/°C. This change is obviously due to the presence of both the epoxy-glue surrounding the sensor and the metallic material of the specimen, as:

$$K^*_{\mathrm{T}} = K_{\mathrm{T}} + K_{\varepsilon}(\alpha_{\mathrm{media}} - \alpha_{\mathrm{SiO_2}}) \tag{11}$$

where α_{media} and $\alpha_{\mathrm{SiO_2}}$ are the coefficients of thermal expansion of the surrounded media and the silica, respectively. The estimated errors on these apparent sensitivities are 0.4 pm/°C and 0.3 pm/°C for LPG and FBG respectively. Using (9), the errors of temperature and strain measured in this conditions can be estimated to be 0.18°C and 4.77 $\mu\varepsilon$. Here again, in order to validate that the cross sensitivities can be neglected, several strain measurements at fixed temperatures (22°C, 76°C and 104°C) are performed. Straight lines close to being strict parallels are obtained, which leads us to conclude that cross-sensitivities are non significant. Finally, the mean value for the strain sensitivity of the LPG over the range 22°C-104°C is found to be $K_{\varepsilon\mathrm{L}}$ = -0.187 pm/$\mu\varepsilon$ with a standard deviation of 0.011 pm/$\mu\varepsilon$. For the FBG, a mean value of $K_{\varepsilon\mathrm{F}} = 1.199$ pm/$\mu\varepsilon$ with a standard deviation of 0.0016 pm/$\mu\varepsilon$ is reported. The small discrepancy between strain calibration for the free sensor or for the embedded sensor can be attributed to the different apparatus and procedures used to submit and measure the strain: in the first case (free sensor), the strain is deduced from the measured force that takes place in the cross-section of the optical fiber and the knowledge of the Young modulus, whereas in the second case (embedded sensor) the strain is measured indirectly via a strain gauge positioned under the specimen surface.

5. Validation

In order to validate the discrimination method presented here, random acquisitions are performed at some imposed strain and temperature levels on the instrumented specimen. Obviously, both temperature and strain are also measured by thermocouple and strain gauge but they are considered unknown in our sensor's point of view.

Using the temperature and strain sensitivities found previously and the wavelength shifts deducted from the optical signal, one might now estimate temperature and strain really measured by the embedded sensor using (2) expressed as:

$$\begin{bmatrix} \Delta T \\ \Delta\varepsilon \end{bmatrix} = [K]^{-1} \begin{bmatrix} \Delta\lambda_{\mathrm{bL}} \\ \Delta\lambda_{\mathrm{bF}} \end{bmatrix} \tag{12}$$

Figure 10 presents the discrepancies between the measured and the prescribed thermal and mechanical loads for numbered tests, which is summed up in table 2.

It is observed that our sensor experimentally well discriminate temperature from strain. In these conditions, maximum errors of 0.5°C and 3 $\mu\varepsilon$ are reported in the range [30°C-100°C; 200 $\mu\varepsilon$-1500 $\mu\varepsilon$], which is a quite good discrimination in view of the estimated errors.

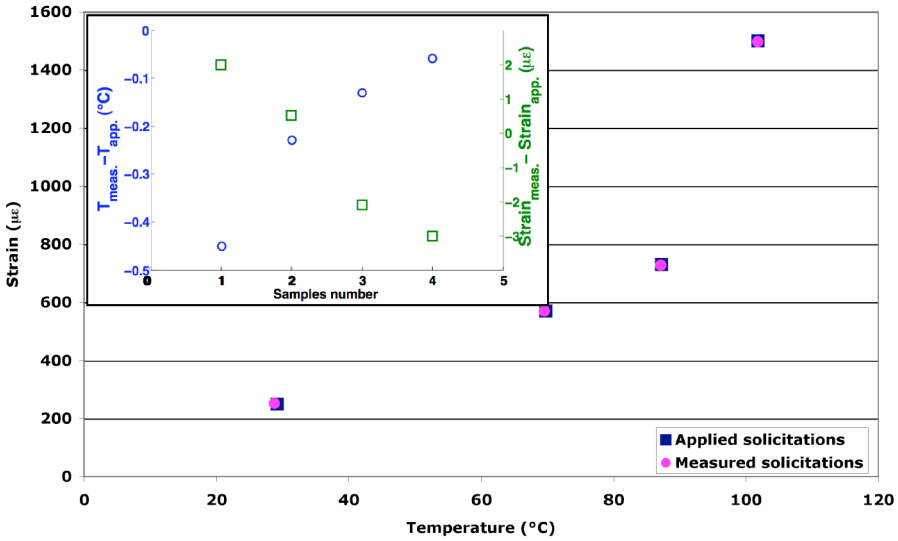

Figure 10. Comparison between simultaneous measured and applied temperature and strain. The inserted graph presents the discrepancies where $T_{meas} - T_{app}$ ($Strain_{meas}$-$Strain_{app}$) stand of the difference between the measured and applied temperature (strain)

Samples #	T_{TC} (°C)	ε_{gauge} ($\mu\varepsilon$)	$\Delta\lambda_{bL}(nm)$	$\Delta\lambda_{bF}(nm)$	T_{meas} (°C)	$\varepsilon_{meas}(\mu\varepsilon)$
1	29.19	250	0.21	0.457	28.74	252.19
2	69.72	570	1.72	1.798	69.49	571.52
3	87.22	730	2.37	2.401	87.09	727.89
4	101.81	1500	2.79	3.656	101.75	1496

Table 2. Discriminated measured temperature and strain by comparison with applied ones

Conclusion

We reported an optical fiber sensor based on dual association of long and short period gratings, which can be used for discrimination of simultaneous strain and temperature measurements at the same spatial position. The developed sensor exhibits a strain sensitivity of $K_{\varepsilon L}$ = -0.208 ± 0.03 pm/$\mu\varepsilon$ and $K_{\varepsilon F}$ = 1.10 ± 0.01 pm/$\mu\varepsilon$ and a temperature sensitivity of K_{TL} = 39.8 ± 0.8 pm/°C and K_{TF} = 13.1 ± 0.3pm/°C. Experiments have been made to find cross-sensitivities negligible, differences found are within errors. The estimated errors of the measured strain and temperature are found to be within 0.4°C and 5 $\mu\varepsilon$.

Our sensor has been embedded in a metallic specimen, where strain and temperature measured by the sensor have been reported to be (K_{TL} = 37.8 ± 0.4 pm/°C, K_{TF} = 23.7 ± 0.3 pm/°C) and ($K_{\varepsilon L}$ = -0.201 ± 0.006 pm/$\mu\varepsilon$, $K_{\varepsilon F}$ = 1.18 ± 0.02 pm/$\mu\varepsilon$). We also take cross-sensitivities into considerations. Strain measurements performed at several temperatures exhibit no differences in sensitivity, which lead to the

conclusion that they are negligible. One stated the discrimination efficiency E in order to compare our technique to those exposed in the literature which highlights the good strain and temperature discrimination values.

Validation of the discrimination for structural health monitoring has been made while performing wavelengths' shifts acquisition at random strain and temperature. The applied solicitations measured by our sensor are within the estimated errors of strain and temperature found with thermocouple and strain gauge.

As for future work, this successfully validated component may be implemented in an in-situ composite fabrication process to monitor the solicitations applied on the material during the process, and after for health monitoring.

References

[1] James S W, Dockney M L and Tatam R P 1996 Simultaneous independent temperature and strain measurement using in-fibre Bragg grating sensors *Elec. Lett.* **32** 1133

[2] Song M, Lee S B, Choi SS and Lee B 1997 Simultaneous Measurement of Temperature and Strain Using Two Fiber Bragg Gratings Embedded in a Glass tube *Optical Fiber Technology* **3** 194

[3] Liu H B, Liu H Y, Peng G D and Chu P L 2003 Strain and temperature sensor using a combination of polymer and silica fibre Bragg gratings *Opt. Commun.* **219** 139

[4] Shu X, Zhao D, Zhang L and Bennion I 2004 Use of dual-grating sensors formed by different types of fiber Bragg gratings for simultaneous temperature and strain measurements *Appl. Opt.* **43** 2006

[5] Xu M G, Geiger H, Dakin J P 1996 Fibre grating pressure sensor with enhanced sensitivity usinga glass-bubble housing *Electron. Lett.* **32** 1996

[6] Song M, Lee S B, Choi S S and Lee B 1997 Simultaneous Measurement of Temperature and Strain Using Two Fiber Bragg Gratings Embedded in a Glass tube*Opt. Fiber Technol.* **3** 194

[7] Zhao Y, Li P, Wang Z and Pu A 2000 A novel fiber-optic sensor used for small internal curved surface measurement *Sensor Actuat. A-Phys.* **86** 211

[8] Frazao O, Marques L, Marques J M, Baptista J M and Santos J L 2007 Simple sensing head geometry using fibre Bragg grafings for strain -temperature discrimination *Opt. Commun.* **279** 68

[9] Xu M G, Han W T, Paek U C Chung Y 1994 Discrimination between strain and temperature effects using dual-wavelength fibre grating sensors *Elec. Lett.* **30** 1085

[10] Echevarria J, Quintela A, Jauregui C and Lopez-Higuera J M 2001 Uniform fibre Bragg grating first-and-second-order diffraction wavelength experminetal characterization for strain-temperature discrimination *IEEE Photonic. Tech. L.* **13** 696

[11] Yam S P, Brodzeli Z, Wade S A, Rollinson C M, Baxter G W and Collins S F 2009 Use of first-order diffraction wavelenths corresponding to dual-grating periodicities in a single fibre Bragg grating for simultaneous temperature and strain measurement *Meas. Sci. Technol.* **20** 034008

[12] Xu M G, Dong L, Reekie L, Tucknott J A and Cruz J L 1995 Temperature-independent strain sensor using a chirped Bragg grating in a tapered optical fibre *Electron. Lett.* **31** 823

[13] Chehura E, James S W and Tatam R P 2007 Temperature and strain discrimination using a tilted fibre Bragg grating *Opt. Commun.* **275** 344

[14] Oh S T, Han W T, Paek U C and Chung Y 2004 Discrimination of temperature and strain with a single FBG based on the birefingence effect *Opt. Express* **12** 724

[15] James S W and Tatam R P 2003 Optical fiber long-period grating sensors: characteristics and application *Meas. Sci. Technol.* **14** 49

[16] Bhatia V, Campbell D and Claus R O 1997 Simultaneous strain and temperature measurement with long-period gratings *Opt. Lett.* **22** 648

[17] Allsop T, Webb D J and Bennion I 2003 A comparison of the sensing characteristics of long period gratings written in three different types of fiber *Opt. Fiber Technol.* **9** 210

[18] Han Y G, Lee S B, Kim C S, Kang J U, Paek U C and Chung Y 2003 Simultaneous measurement of temperature and strain using long period fiber gratings with controlled temperature and strain sensitivities *Opt. Express* **11** 476

[19] Patrick H J, Williams G M, Kersey A D, Pedrazzani J R and Vengsarkar A M 1996 Hybrid Fiber Bragg Grating Long Period Fiber Grating Sensor for Strain/Temperature Discrimination *IEEE Photonic. Tech. L.* **8**

[20] Guan B O, Tam H Y, Tao X M and Dong X Y 2000 Simultaneous Strain and Temperature Measurement Using a Superstructure Fiber Bragg Grating *IEEE Photonic Tech. L.* **12** 675

[21] Bey A K, Sun T and Grattan K 2008 Simultaneous measurement of temperature and strain with long period grating pairs using low resolution detection *Sensors and Actuators A* **144** 83

[22] Wang M, Li T, Zhao Y, Wei H, Tong Z and Jian S 2001 Simultaneous measurement of strain and temperature using dual-period fiber grating *Proc. SPIE* **4579** 265

[23] Bhatia V 1999 Applications of long-period gratings to single and multi-parameter sensing *Opt. Express* **4** 457

[24] Gangopadhyay T K, Paul M C and Bjerkan L Fiber-optic sensor for real-time monitoring of temperature on high voltage (400kV) power transmission lines *Proc. SPIE* **7503**

[25] Neuilly M 1987 Erreurs de mesure *Techniques de l'ingénieur, traité Mesure : généralité* **R280** 1

[26] Miao B, Liu Y and Zhao Q 2008 Simultaneous measurement of strain and temperature using tilted fibre Bragg grating *Elec. Lett.* **44**

[27] Brady G P, Kalli K, Webb D J, Jackson D A, Reekie L and Archambault J L 1997 Simultaneous measurement of strain and temperature using the first- and second-order diffraction wavelengths of Bragg gratings *IEE Proc.-Optoelectron.* **144** 156

[28] Allsop T, Zhang L, Webb D J and Bennion I 2002 Discrimination between strain and temperature effects using first and second-order diffraction from a long-period grating *Opt. Commun.* **211** 103

[29] Farahi F, Webb D J, Jones J D C and Jackson D A 1990 Simultaneous Measurement of Temperature and Strain: Cross-Sensitivity Considerations *J. Lightwave Technol.* **8** 138